Phase and amplitude fluctuations near TI in the incommensurate phase of Rb2ZnCl4 : Mn2+ through E.P.R. investigations

A. Kaziba, J.C. Fayet

J. Physique **47** (1986) 239-248 FÉVRIER **1986**, PAGE 239

Classification
Physics Abstracts
61.16N

Phase and amplitude fluctuations near T_I in the incommensurate phase of Rb_2ZnCl_4 : Mn^{2+} through E.P.R. investigations

A. Kaziba and J. C. Fayet

Laboratoire de Spectroscopie du Solide (*), Faculté des Sciences, Route de Laval, 72017 Le Mans Cedex, France

(*Reçu le 15 juillet 1985, accepté le 30 septembre 1985*)

Résumé. — Un traitement numérique des spectres expérimentaux de la sonde Mn^{2+} nous a permis d'éliminer la structure hyperfine et de révéler la forme des raies de structure fine dans la phase incommensurable au voisinage de T_I. Nous l'analysons par un modèle simple mettant en jeu l'amplitude critique, la phase locale de la modulation statique et les densités spectrales de leurs fluctuations. Nous concluons à l'existence de fluctuations de phase de grande amplitude, près de T_I, qui se durcissent pour atteindre un régime stationnaire au-dessous de (T_I − 4 K) caractérisé par une densité spectrale substantielle dans le domaine de fréquence 10^{10} s^{-1}.

Abstract. — A computer treatment of the experimental spectra of the Mn^{2+} probe enables us to eliminate the irrelevant hyperfine structure and to reveal the shape of the fine structure lines in the incommensurate phase near T_I. We analyse it by a simple model taking into account the critical amplitude, the local phase of the modulation wave and the spectral densities of their fluctuations. We conclude with the existence of large phase fluctuations near T_I which tighten to reach below (T_I − 4 K), a stationary regime marked by a substantial spectra density in the 10^{10} s^{-1} frequency range.

Introduction.

Rb_2ZnCl_4, like other compounds in the A_2MX_4 series including K_2SeO_4, exhibits P_{nma} symmetry in the high temperature normal phase and, at $T_I \simeq 30$ °C, undergoes a structural transition to an incommensurate phase characterized by a wave-vector $\mathbf{k}_I = \frac{1}{3}(1 - \delta)\,\mathbf{a}^*$ [1-3].

According to a simple model, one component of the order parameter — the phase of the modulation — would exhibit a characteristic excitation spectrum associated with a « pseudo-acoustic » phonon : the phason mode with a zero gap at $q = \mathbf{k}_I$. Actually, this mode has been directly observed in K_2SeO_4 [4, 16] by inelastic neutron scattering, but far from T_I and far from $\mathbf{k}_I$. In Rb_2ZnCl_4 and related compounds, overdamping and probable order-disorder character of the transition make inelastic scattering inefficient for accurate investigations. Diffuse X-ray Bragg scattering in Rb_2ZnCl_4 permitted to locate an upper limit of the phason gap at 1.2×10^{10} s^{-1} [3].

Unlike a true acoustic phonon with $\omega \to 0$ as $q \to 0$, low frequency phase fluctuations centred at $q \neq 0$ induce a modulation of the local crystal field [5]. Consequently, they can strongly influence the magnetic resonance line of a spin probe at some crystal site of the incommensurate lattice. For instance, they are responsible for drastic motional averaging effects leading to a persistent « commensurate-like » N.M.R. [6] or E.P.R. [7] line below T_I or for an anomalously high value of the effective critical exponent β [8], and also for a particular behaviour of the relaxation time $T_{1,\phi}$, which monitors the spectral density $J_{1,\phi}$ for $\omega = \omega_L \simeq 10^8$ s^{-1} in N.M.R. spectroscopy [9]. By measuring the spin-lattice relaxation time $T_{1,\phi}$ in $|N(CH_3)_4|_2ZnCl_4$ [10], Rb_2ZnCl_4 [9] and Rb_2ZnBr_4 [6] above and below the lock-in transition at T_c, Blinc was able to locate the phason gap, in these incommensurate phases in the 10^{11}-10^{12} s^{-1} frequency range.

In this paper we attempt to complete, the analysis of the critical amplitude of the modulation and of the spectral density of fluctuations by considering the line shape of an E.P.R. probe : the Mn^{2+} ion substituted for Zn^{2+}. We assume that the probe which fits the host closely, correctly mirrors the essential qualitative features of the bulk. We shall also emphasize that the E.P.R. measurements show important modifications of the E.S.R. line in a small temperature range around T_I. We shall follow the

(*) U.A. n° 807.

underlying phenomena by varying the temperature smoothly.

1. Theoretical background.

The critical displacement field in a 1-D modulated structure can be represented by

$$u_i^\alpha = A(a_i^\alpha \cos\theta \cos\phi_i + b_i^\alpha \sin\theta \sin\omega_i).$$

$A \propto (T_I - T)^\beta$ is the critical amplitude ($\beta = 0.36$); $\alpha = x, y, z$. The index l indicates the type of the atom i. a_l^α and b_l^α represent the eigenstates of two displacement modes coupled in quadrature. θ is the coupling parameter. This coupling is generally involved in an incommensurate phase [11, 12]. ϕ_i, the local phase of the static modulation, is given by $\phi_i = \mathbf{k}_I \cdot \mathbf{r}_i + \phi_0$. ϕ_0 is constant in the plane wave regime; $\mathbf{k}_I$ is the incommensurate wave vector.

Let us consider a spin probe at site i, with $S > 1/2$ and with an isotropic invariant g factor. A resonance line centred at $H = H_0$ in the normal (N) phase is shifted by the modulation wave according to [13] :

$$\Delta H(\phi_i) = Ah_1 \cos(\phi_i + \phi_1) + \\ + A^2(h_2' + h_2'' \cos 2(\phi_i + \phi_2))$$

which is nothing but a power expansion limited to second order with respect to the amplitude of the modulation. It is worth outlining the mechanisms which are responsible for the local line shift $\Delta H(\phi_i)$. The displacements of atom i and atoms j within the range of the probe modify the spin-lattice interaction to first and second order, according to

$$\Delta\mathcal{H} = \sum_K \mathcal{H}_1^K u_K^\alpha + \sum_{K,K'} \mathcal{H}_2^{K,K'} u_K^\alpha u_{K'}^\beta = \\ = A_{(T)} \mathcal{H}_1 + A_{(T)}^2 \mathcal{H}_2 \\ K, K' = i, j. \qquad (1)$$

It is essential to note that sine and cosine functions with different phases are involved in this expression.

The $\mathcal{H}_1^K$'s and $\mathcal{H}_2^{KK}$'s represent spin operators involving the microscopic details of the interaction with the individual atomic displacements. The spin-Hamiltonian in the incommensurate phase is given by

$$\mathcal{H}(T < T_I) = \{ g\beta\mathbf{H} \cdot \mathbf{S} + \mathcal{H}_0(T) \} + \Delta\mathcal{H}. \quad (2)$$

The first term $\{ \ldots \}$, associated with the normal phase, defines a set of eigenstates $| m \rangle$ and the resonance field H_0 for a particular transition $| 1 \rangle \rightarrow | 2 \rangle$. $\Delta\mathcal{H}$ can be treated as a perturbation of $\mathcal{H}_0$. $\mathcal{H}_0$, and, consequently, H_0 may eventually exhibit an irrelevant thermal drift.

To first order, the relevant linear line shift in expression (1) involves only the diagonal matrix elements of the $\mathcal{H}_1^K$'s with different local phase factors : $\cos\phi_K$, $\sin\phi_K$. Such a sum of terms can be set in the form given in (1) through a convenient choice of ϕ_1. The parameter h_1 depends on **H** but does not depend on T. The linear term can be forbidden by symmetry for **H** along symmetry elements of the (N) phase. Then $\mathcal{H}_1^K$ has no diagonal matrix-elements on the $| m \rangle$ basis. Therefore, at first order, $\mathcal{H}_1^K$ cannot be responsible for any secular effect.

Similarly, the quadratic line shift in (1) involves off-diagonal elements of $\mathcal{H}_1^K$ at second-order perturbation and diagonal matrix elements of $\mathcal{H}_2^{KK'}$ at first-order perturbation. A convenient choice of ϕ_2 leads to the expression in (1), with h_2' and h_2'' depending on **H** but independent of T. It turns out that the local line shift cannot be easily connected to the local phase ϕ_i except under particular circumstances. If Local and Single Mode contributions are dominant (L.S.M. approximation), we obtain $\phi_1 = \phi_2$. The quadratic shift is reduced to $A^2 h_2 \cos^2\phi$. i.e. $h_2' = h_2''$, or $\left| \frac{h_2' + h_2''}{2 h_2''} \right| = 1$. This ratio can be used as an estimation of the validity of the L.S.M. approximation.

Finally, the shape of the experimental line is given by

$$F(H) = \int_0^{2\pi} f\left\{ \frac{H - H(\phi_i)}{L} \right\} d\phi_i \qquad (3)$$

and is marked by singularities located at $H = H(\phi_i)$ such that $\frac{dH(\phi_i)}{d\phi_i} = 0$. f and L represent background line shape and line width which are irrelevant to the phase transition.

If the linear term is dominant, we obtain two symmetrical singularities at $H = H_0 \pm Ah_1$ associated with $\phi_i + \phi_1 = 0, \pi$. If the linear term is forbidden, we obtain two singularities located at $H = H_0 + A^2(h_2' \pm h_2'')$ corresponding to $\phi_i + \phi_2 = (0, \pi)$, and $\left(\pm \frac{\pi}{2}\right)$ respectively.

Much more complicated line shapes are obtained generally. They have been discussed [13] and experimentally obtained [7] elsewhere.

We have not yet considered amplitude and phase fluctuations, which may affect the E.P.R. spectra near T_I. We shall therefore set $A(t) = A(T) + \delta A(t)$ and $\phi_i(t) = \phi_i + \delta\phi(t)$, δA and $\delta\phi$ represent fluctuations with a correlation length much larger than the range of the probe. Now we have to deal with a local time-dependent spin-Hamiltonian :

$$\mathcal{H}(\phi_i, t) = \langle \mathcal{H}(\phi_i, t) \rangle + \{ \mathcal{H}(\phi_i, t) - \langle \mathcal{H}(\phi_i, t) \rangle \}.$$

The time averaged term determines the centre of the local line. The time dependent term $\{ \ldots \}$ defines the local line shape and the local line width through secular and non secular mechanisms. The non-secular line broadenings are closely related to the relaxation times $T_{1,A,\phi}$ and the relaxation paths may be very complicated [13].

For our purpose we shall limit ourselves to simplified situations corresponding to particular experimental conditions.

a) Let us consider large phase fluctuations with a Gaussian probability distribution characterized by $\langle \delta\phi_{(t)}^2 \rangle = \sigma^2$. Let us assume motional averaging, i.e. fast enough fluctuations.

The averaged local line shift is derived from [13]

$$\langle \Delta H(\phi_i) \rangle = Ah_1 \, e^{-\sigma^2/2} \cos(\phi_i + \phi_1) + \\ + A^2 \{ h_2' + h_2'' \, e^{-2\sigma^2} \cos 2(\phi_i + \phi_2) \} .$$

In the thermodynamic limit, not too close to T_I, we may set [8] $\sigma^2 = \sigma_0^2 (T_I - T)^{-2\beta}$.

The effect of these fluctuations is a reduction of the local line shift particularly for the quadratic contribution. This may lead to an apparently anomalously large value of the critical exponent β [8] or, ultimately to a « commensurate-like » line below T_I [6, 7]. Practically, this may preclude an accurate determination of T_I with the resonance measurements.

b) Let us assume that the L.S.M. approximation is valid. For a small amplitude of the modulation wave we obtain

$$\mathcal{H}(\phi_i, t) = g\beta \mathbf{H} \cdot \mathbf{S} + \mathcal{H}_0 + (A + \delta A)\,\mathcal{H}_1 \cos(\phi_i + \delta\phi) \\ = \{ g\beta \mathbf{H} \cdot \mathbf{S} + \mathcal{H}_0 + A\mathcal{H}_1 \cos\phi_i \langle \cos\delta\phi \rangle \} + \delta A\, \mathcal{H}_1 \cos\phi_i - \\ - \delta\phi\, A\mathcal{H}_1 \sin\phi_i - \left\{ \frac{\delta\phi^2 - \langle \delta\phi^2 \rangle}{2} \right\} A\mathcal{H}_1 \cos\phi_i . \qquad (4)$$

When the linear local line shift is forbidden by symmetry, $\mathcal{H}_1$ contributes, to first order, to non-secular broadenings only. We obtain

$$L_{n.s}(\phi_i) = L_A(\langle \omega \rangle) \cos^2\phi_i + L_\phi(\langle \omega \rangle) \sin^2\phi_i . \qquad (5)$$

The parameters $L_{A,\phi}(\langle \omega \rangle)$ monitor the behaviour of the spectral densities $J_{1,A,\phi}(\langle \omega \rangle)$, where $\langle \omega \rangle$ represents the average of energy differences between spin levels involved in the relaxation paths. For our measurements, $\langle \omega \rangle$ is in the range of 10^{10} Hz, typically two orders of magnitude larger than the frequency range involved in T_1 measurements by N.M.R. spectroscopy [9]. In this mechanism, the amplitude fluctuations contribute to widen the singularity at $\phi_i = (0, \pi)$, and the phase fluctuations affect the singularity at $\phi_i = \left(\pm \frac{\pi}{2} \right)$. We have neglected contributions from $J_{2,\phi}(\langle \omega \rangle)$, which may arise through the term $(\delta\phi^2 - \langle \delta\phi^2 \rangle)$. This approximation is valid for either small amplitude fluctuations or for a large damping of these fluctuations as in Rb_2ZnCl_4.

When the linear local shift is dominant, a similar analysis can be made. The essential difference is a secular contribution of $\mathcal{H}_1$, which now has diagonal matrix elements. In the fast fluctuation regime, we obtain

$$L_s(\phi_i) = L_A(0) \cos^2\phi_i + L_\phi(0) \sin^2\phi_i . \qquad (6)$$

The parameters $L_{A,\phi}(0)$ involve the diagonal matrix elements of $\mathcal{H}_1$ and the spectral densities $J_{1,A,\phi}(\omega \cong 0)$.

The amplitude fluctuations widen the edge singularities at $\phi_i = 0, \pi$. The relevant parameter is the spectral density $J_{1,A}(0)$. The phase fluctuations have their maximum effect for $\phi_i = \pm \frac{\pi}{2}$ — that is, in the flat part of the incommensurate line. They can hardly be evidenced from a visual examination of the line shape.

It turns out that phase and amplitude fluctuations influence the line shape. The « static » line shape given by expression (3) has to be substituted for by

$$F(H) = \int_0^{2\pi} f\left\{ \frac{H - \langle H(\phi_i) \rangle}{L(\phi_i)} \right\} d\phi_i . \qquad (7)$$

The local line position $\langle H(\phi_i) \rangle$ and the phase dependent local linewidth $L(\phi_i)$ include dynamical parameters, as evidenced by the simple model described just above.

2. Computer treatment of the experimental spectra. Preliminary results.

We have studied the E.P.R. line associated with the high magnetic field electronic transition $\left(M_s = \frac{3}{2} \rightarrow \frac{5}{2} \right)$ for $\mathbf{H} /\!/ \mathbf{a}$ and $\mathbf{H}$ in the a-b plane with $\sphericalangle (\mathbf{H}, \mathbf{a}) = 4° 20'$. For these orientations, the Zn^{2+} sites are equivalent in the (N) phase, and the main quadrupolar axis Z ($\sphericalangle (Z, \mathbf{a}) = 7°$ with Z in the a-c plane above T_I) stays in the vicinity of $\mathbf{H}$, for limited amplitude of the displacement field in the (INC) phase (near T_I). The line does not overlap with other fine structure lines. On the other hand, for this transition the Zeeman effect is predominant and the forbidden hyperfine line ($\Delta M_I \neq 0$) has no significant intensity : the hyperfine structure is a simple sextuplet ($\Delta M_I = 0$) not much influenced by second-order effects and not

very sensitive to the structural phase transition. Therefore, the line shape below T_I is given by

$$F_{exp} = F_q * S_{hyp} \quad (8)$$

* denotes a convolution, and F_q represents the distribution of the quadrupolar local line shifts due to the incommensurate modulation. S_{hyp} is a background hyperfine sextuplet which is nearly the same for all the magnetic field orientations considered. The irrelevant characteristics of S_{hyp} (line width, line shape and line splittings) can be determined in the uncritical temperature region above T_I.

The relevant modifications of the E.P.R. spectra can be monitored by F_q. Typical shapes of F_q obtained by a computer deconvolution of F_{exp} by S_{hyp} using a fast-Fourier transformation program, are represented in figure 1 for **H**//**a**, $\sphericalangle$ (**H**, **a**) = 40′ and $\sphericalangle$ (**H**, **a**) = 4° 20′ respectively. This procedure enables us to immediately determine the essential features of the distribution of the local quadrupolar line shift otherwise obscured by the hyperfine interaction (Fig. 1o).

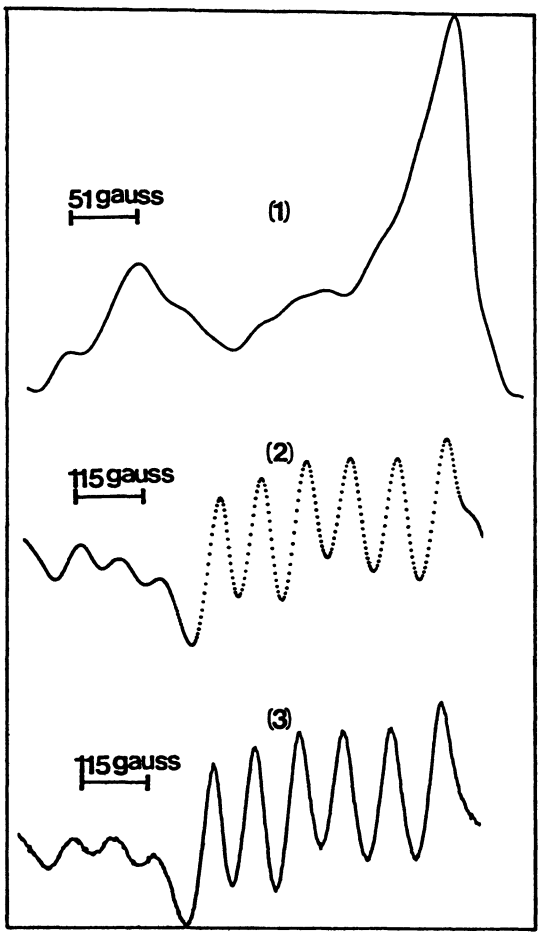

Figure 1 o

Fig. 1. — Typical shapes of F_q obtained by a computer deconvolution of the experimental spectra by the hyperfine structure.
(o) *Principle* : (3) bottom : experimental spectrum. One scarcely distinguishes two overlapping, distorted, hyperfine sextuplets ; (1) top F_q obtained by deconvolution ; (2) middle : back-calculation of the experimental spectrum used as a control of the procedure. a) **H**//**a** ; b) $\sphericalangle$ (**H**, **a**) = 40′ ; c) $\sphericalangle$ (**H** ; **a**) = 4° 20′.

From a visual examination of the curves $F_q(T, \mathbf{H})$ in figures 1, we obtain the following preliminary results.

2.1 **H**//**a** ; $T < T_I - 4$ K. — $F_q(T)$ exhibits two edge singularities. That of the high field is nearly stationary at $H_0(T < T_I) \simeq H_0(T > T_I)$. By cooling, the low-field singularity is progressively shifted to low magnetic fields. For this orientation, the local line shift depends quadratically on the amplitude of the modulation wave according to symmetry. A dominant L.S.M. contribution to the local line shift can be inferred from the nearly stationary position of the high field singularity which would correspond to $\phi_i = \pm \frac{\pi}{2}$. An important feature is the asymmetry of the singularities (Fig. 1a). This cannot be explained by a rigid modulation wave.

2.2 $\sphericalangle$ (**H**, **a**) = 4° 20′. — We obtain two asymmetric singularities. Cooling shifts one to high fields, the other to low fields. The linear shift is dominant for this orientation. A smaller quadratic term is responsible for the asymmetry of the singularities. We apparently obtain a normal and simple result. Actually, the

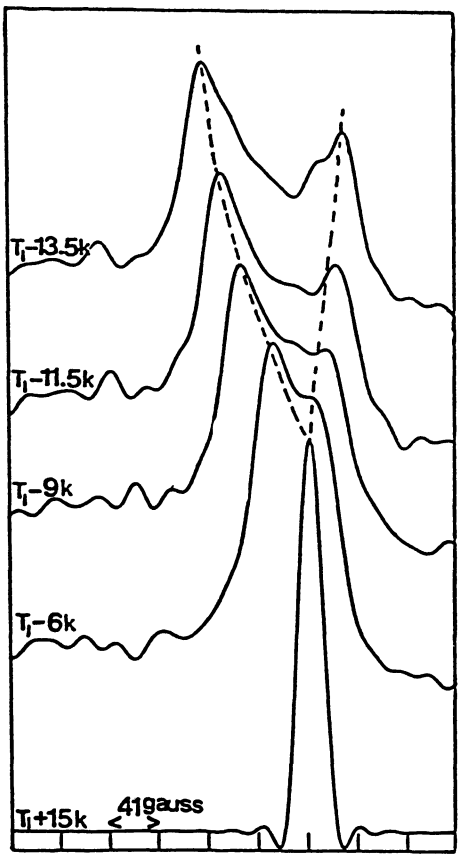

Figure 1 a

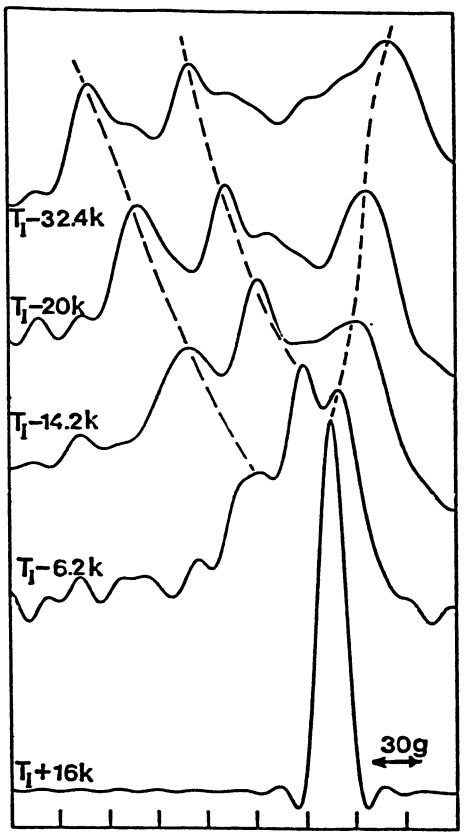

Figure 1 b

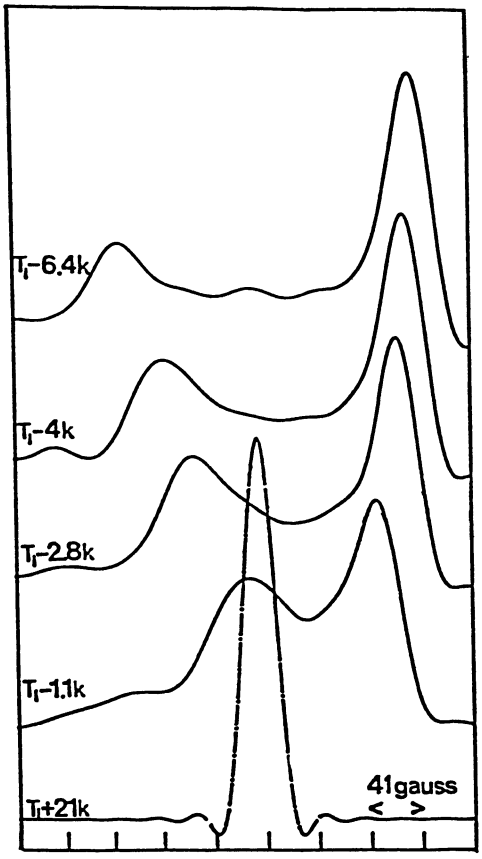

figure 1 c

forthcoming detailed examination of the shape of F_q for **H**//**a** and $\sphericalangle$ (**H**, **a**) = 4° 20′ is the object of the present paper.

2.3 $\sphericalangle$ (**H**, **a**) = 40′. — The very small tilt of **H** away from **a** induces a small linear contribution to the local line shift according to symmetry. We obtain three singularities. With respect to **H**//**a**, the third singularity occurs essentially through a linear splitting of the low-field singularity ($\phi = 0, \pi$) by the linear term. We shall not discuss this result, which shows the reliability and the sensitivity of the deconvolution procedure, further, except to note that this procedure leads to a loss of resolution. Indeed, to avoid spurious signals arising from recording noise and from the tails of the experimental lines, we had to use a filtering function to cut off the high « frequency » components of the Fourier transforms. Therefore, we have used a second procedure based upon the theoretical model outlined in section 1. The parameters defining the local line shift and the local line width were adjusted to obtain an accurate reconstruction of the experimental line with the help of a convolution program.

At low temperature, the local line shifts are large, and there is no problem about the resolution. The two procedures give consistent results for F_q. Near T_I, the deconvolution procedure is inoperative due to the loss of resolution. The second procedure enables us to make a more accurate analysis of the quadrupolar line shape, but through a theoretical model.

A different experimental difficulty arises in the determination of the critical temperature T_I, whatever the sensitivity of the paramagnetic probe. Indeed, it is now well-known [6-8] that the phase fluctuations with a large amplitude near T_I average the « incommensurate » resonance line, more or less. This effect delays the appearance of clearly resolved edge singularities which identify the incommensurate phase. Therefore, to determine T_I, we have used the experimental line corresponding to the electronic transition $M_s = -\frac{1}{2} \rightarrow \frac{1}{2}$, for which the « forbidden » hyperfine ($\Delta M_I = \pm 1, \pm 2$) lines have the largest intensity and are very sensitive to the tilts of the quadrupolar axes induced by the breaking, below T_I, of the point symmetry of the Zn^{2+} sites [14]. For **H**//**a**, these « forbidden » hyperfine lines exhibit a sharp increase at a temperature T_I' which can be determined with an accuracy of 0.1 K. We have set $T_I' = T_I$ by postulating that the behaviour of the forbidden lines was not affected by the critical dynamics. T_I' is the highest temperature for which we were able to detect the phase change. We found that T_I' was dependent on the Bridgmann badges from which we obtained the E.P.R. samples.

To summarize, all the details about the quadrupolar local shifts and the local lines widths have been obtained with the help of a computer treatment of the experimental signal to eliminate the hyperfine struc-

ture which obscures the essential features of the dependence on temperature of the quadrupolar effects.

The deconvolution procedure is rapid and independent of any theoretical model, but a low resolution makes it inefficient near T_I. The convolution procedure permits a more accurate investigation near T_I, but it requires the help of some theoretical model. The validity of this model can be checked at low temperatures where the resolution of the deconvolution procedure is sufficient. The two procedures are therefore complementary.

3. Results of the E.P.R. spectra simulations

3.1 **H//a** : SAMPLE A. — For this sample, we have found $T_I = T_I' = 302.7$ K. Below $T_I - 4$ K, the deconvolution procedure indicates two well-resolved singularities (Fig. 1a). The distance between the singularities does not obey the critical law $\Delta H_{\parallel} \propto (T_I - T)^{2\beta}$ ($\beta = 0.36$). Moreover, the high-field singularity $\left(\phi = \pm \frac{\pi}{2}\right)$, the position of which is smoothly dependent on T, is less sharp than the low-field singularity (Fig. 1a). Guided by the theoretical model of § 1, we have set

$$L(\phi_i) = L_A^P \cos^2 \phi_i + L_\phi^P \sin^2 \phi_i \quad (\text{P for } \mathbf{H//a})$$

$$\Delta H(\phi_i) = g_2' + g_2'' \cos 2\phi_i \qquad (9)$$

$$F_q(H) = \int_0^{2\pi} f\left\{\frac{H - \Delta H(\phi_i)}{L(\phi_i)}\right\} d\phi_i$$

with f intermediate between a Lorentzian and a Gaussian line shape.

Fitting the parameters L_A^P, L_ϕ^P, g_2' and g_2'', we could accurately reconstruct the shape of F_q obtained by deconvolution below $T_I - 5$ K, and we found $L_A^P < L_\phi^P$.

To obtain more resolution near T_I, we have used the same model, but we have fitted the parameters by using a convolution procedure for the temperature range (T_I, $T_I - 20$ K). The experimental spectra is given by (Eq. (8)).

In this way we were able to determine an « edge singularity » structure for F_q, i.e. $g_2'' \neq 0$, up to ($T_I - 1$ K). Above this temperature we were unable to discriminate between an « incommensurate » and a « commensurate-like » line shape.

The positions of the singularities given by $g_2' \pm g_2''$ are represented in figure 2 down to ($T_I - 17$ K). We have also represented the centre of the commensurate line above T_I.

The fit of the local line width parameters indicates that L_A^P decreases continuously below T_I, and that L_A^P increases up to a stationary value below ($T_I - 3$ K). A crossover ($L_A^P > L_\phi^P$) → ($L_A^P < L_\phi^P$) occurs at nearly ($T_I - 4$ K). The behaviour of L_ϕ^P, which represents the local line width for $\phi_i = \pm \frac{\pi}{2}$, has a particular interest.

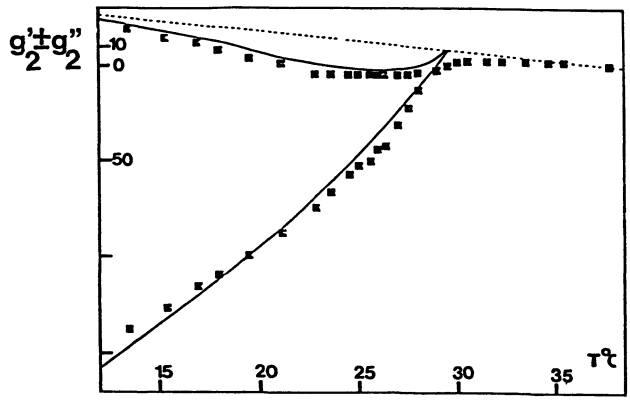

Fig. 2. — Temperature dependence of the « edge singularities » for **H // a** (sample A). The straight line which represents the non critical thermal drift above ($T_I + 8$ K) has been extrapolated to low temperatures to serve as a base line. The full curves represent the calculated positions in the case of large phase fluctuations (see text).

Indeed, line widths generally decrease below the critical temperature.

To confirm this point, we carefully reexamined the line shape applying the deconvolution procedure using a broad-band filtering function to improve the resolution. The counter part was an important noise on the base line (Fig. 3). Nevertheless we could unambiguously observe the broadening of the singularity at $\phi_i = \pm \frac{\pi}{2}$, the sharpening of the singularity at $\phi_i = 0, \pi$, and the crossover near $T = (T_I - 4$ K), all this independent of any theoretical model.

3.2 **H//a** AND $\sphericalangle$ **(H, a)** = 4° 20′ : SAMPLE B. — In a second set of experiments we observed the line shape for **H//a** and $\sphericalangle$ **(H, a)** = 4° 20′ in order to study the linear shift and the quadratic shift in the course of the same temperature treatment for the same sample.

For the sample which was used, we found $T_I' = T_I = 31.8$ °C. Moreover, the temperature range of investigation was limited to $T > (T_I - 8$ K) due to large linear local line shifts. Indeed, below this temperature, the line corresponding to the fine structure 1/2 → 3/2 tends to overlap with the line 3/2 → 5/2 for $\sphericalangle$ **(H, a)** = 4° 20′, precluding a valid treatment of the signal.

For **H//a**, we observed the same qualitative features as for sample A. The results of the fit of L_A^P and L_ϕ^P are represented in figure 4. The positions of the edge singularities are reported in figure 5.

For $\sphericalangle$ **(H, a)** = 4° 20′, using the model

$$\Delta H(\phi_i) = g_1^d \cos \phi_i + g_2^d \cos^2 \phi_i$$

(d for deviation from **H//a**)

$$L^d(\phi_i) = L_A^d \cos^2 \phi_i + L_\phi^d \sin^2 \phi_i$$

we could obtain an accurate computer reconstruction of the experimental line shape. We obtained no

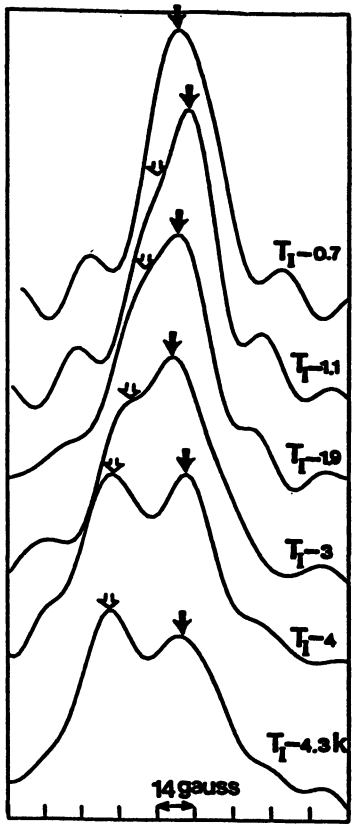

Fig. 3. — Resonance field distribution near T_I, obtained by a computer deconvolution (sample B) with a broad band filtering function. The external magnetic field is directed along **a**. Full arrow : singularity for $\phi = \pm \frac{\pi}{2}$; Open arrow : singularity for $\phi = 0, \pi$. The base line is spoiled by random oscillation due to broad band filtering, which does not prevent us from distinguishing, a crossover between the widths of the singularities. The same features are observed for sample A.

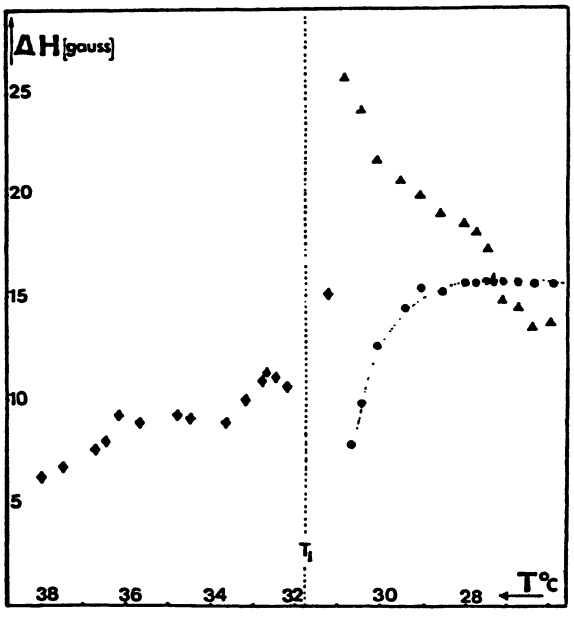

significant improvement by introducing non-local effects (i.e. $\phi_1 \neq \phi_2$). The phase-dependent line width was necessary to obtain a satisfactory computer reconstruction of the experimental lines.

The results for g_1^d and g_2^d are represented in figure 6.

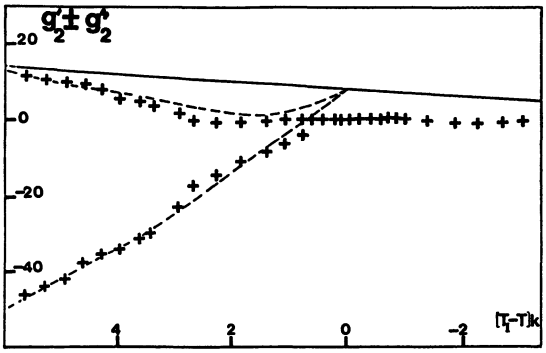

Fig. 5. — Evolution of the line positions with temperature, **H** // **a** (sample B). + : Positions obtained by the spectra simulation. (---) : Fitted positions with the model based on large phase fluctuations and motional averaging. —— : Thermal drift above (T_I + 8 K) extrapolated to low temperatures.

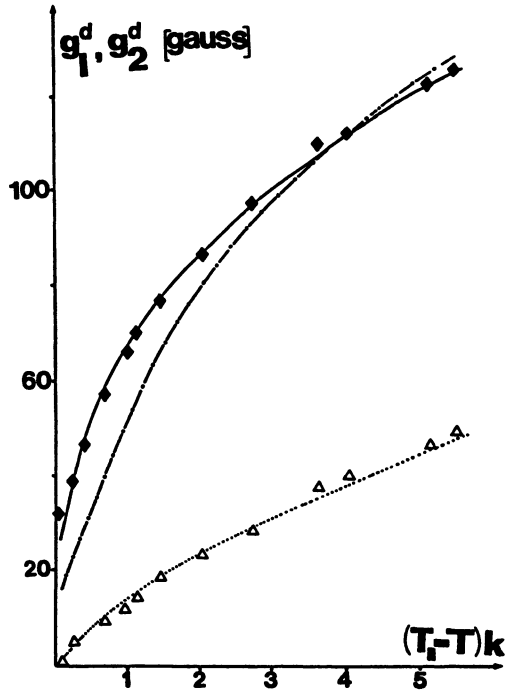

Fig. 6. — Temperature dependence of the position parameters obtained by fitting the experimental spectra : ◆ : g_1^d; △ : g_2^d. Full line : static critical behaviour : $g_1^d \propto (T_I - T)^{0.36}$ according to the theory. Slashed line $g_1^d \propto \varepsilon^\beta \exp\left(-\frac{\langle \phi_0 \rangle^2}{4} \varepsilon^{-\beta}\right)$ according to the motional averaging model : $\langle \phi_0^2 \rangle = 2.5 \times 10^{-2}$.

◀ Fig. 4. — Temperature dependence of the line widths for **H** // **a** (sample B). ◆ : Critical broadening above T_I. ◆ : $T_I - 1\text{K} < T < T_I$: width of the « commensurate-like » line. ▲ : $T < T_I - 1$ K line width of the low magnetic field singularity ($\phi + \phi_2 = 0, \pi$). ● : $T < T_I - 1$ K line width of the singularity at $\phi + \phi_2 = \pm \frac{\pi}{2}$.

The parameters of the local line width L_A^d and L_ϕ^d are represented in figure 7, where we have also represented the line width above T_I.

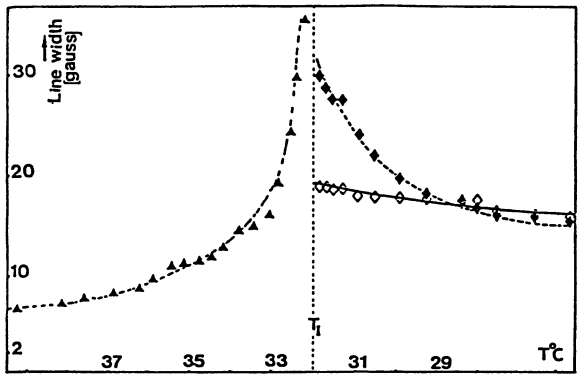

Fig. 7. — Local line widths. Above T_I : (▲). Below T_I : (◆) $\phi = 0, \pi$; (◇) : $\phi = \pm \frac{\pi}{2}$.

The parameter g_1^d, which is the dominant contribution, will be used to study the thermal behaviour of the linear line shift.

4. Discussion.

4.1 **H//a.** — For **H//a** and from $(T_I + 20\,K)$ to $(T_I + 8\,K)$, the centre of the line exhibits a linear thermal drift towards high magnetic fields which can be associated with the lattice contraction and other irrelevant thermal effects. We have extrapolated this linear thermal drift to low temperatures and used it as a base line to evaluate the specific effects of the modulation wave below T_I (Fig. 2).

From $T_I + 8\,K$ to T_I, the centre of the line is stationary. Indeed, the irrelevant thermal drift to high fields is compensated for by critically increasing fluctuations of the ordering coordinate. More details about the critical behaviour above T_I have been given in reference [15].

At T_I, the centre of the line exhibits an evolution towards low fields.

Below $T_I - 1\,K$, the computer reconstruction of the experimental line shape is significantly improved by using a « two-edge singularities » structure. The position of these singularities with respect to the base line (Fig. 2) can be satisfactorily accounted for by the law

$$\Delta H(\pm) = C\varepsilon^{2\beta}(0.8 \pm e^{-\{\phi_0^2 \varepsilon^{-2\beta}\}})$$

with $\phi_0^2 = 3.2 \times 10^{-2}$ and $\varepsilon = \dfrac{T_I - T}{T_I}$ in accordance with an averaging and a Gaussian distribution of phase fluctuations.

For $(T_I - 1\,K)$, we find $(\langle \delta\phi^2 \rangle)^{1/2} = 57°$ in agreement with the N.M.R. results through the same theoretical model for samples grown from aqueous solutions.

On the other hand, the ratio $\left|\dfrac{g_2' + g_2''}{2\,g_2''}\right| = 90\,\%$ indicates that the L.S.M. contributions are more likely dominant. These results support the validity of the simple model for line broadenings described in section 1.

Then, the increase of the local line width parameter L_ϕ^P from $(T_I - 1\,K)$ to $(T_I - 4\,K)$ would indicate a progressive increase of the spectral density $J_{1,\phi}(\langle \omega \rangle)$ ($\langle \omega \rangle \simeq 10^{10}$ Hz) up to a stationary and substantial value. This is an unusual behaviour.

In contrast, the local line width parameter L_A^P evidences a normal decrease associated with a fast hardening beyond 10^{10} Hz of amplitude fluctuations, as in any normal soft mode. Below $(T_I - 10\,K)$, the parameter L_A^P exhibits a stationary value at 10 G above the irrelevant background estimated at $T_I + 20\,K$.

A previous analysis of the line widths above T_I for **H//a** shows that nonsecular broadenings are also dominant in this temperature range [15].

For sample B, we found a different critical temperature — $T_I = 305\,K$ — and a slightly different amplitude of phase fluctuations — $(\langle \delta\phi^2 \rangle)^{1/2} = 50°$ — with the ratio for the L.S.M. contribution being 85 %. The critical temperature seems very sensitive to defects or internal strains, but the essential qualitative features of the spectra are the same in crystals A and B.

4.2 $\sphericalangle$ (**H**, **a**) = 4° 20. — The behaviour of the linear shift g_1^d does not deviate significantly from a static critical behaviour, $g_1^d \propto (T_I - T)^\beta$. We found $\beta = 0.38 \pm 0.04$, which compares with the theoretical value $\beta = 0.36$ (Fig. 6).

Assuming averaging of phase fluctuations with a mean square amplitude $(\langle \phi_0^2 \rangle)_B = \left(\dfrac{\langle \delta\phi^2 \rangle_B}{T_I^{2\beta}}\right) = 2.5 \times 10^{-2}$ as estimated above for **H//a**, we would obtain

$$g_1^d \propto \varepsilon^\beta \exp\left(-\left\{\frac{\langle \phi_0^2 \rangle_B}{4}\,\varepsilon^{-2\beta}\right\}\right);\ \varepsilon = \frac{T_I - T}{T_I}.$$

The results are plotted in figure 6. They show a significant departure from the experimental results in the temperature range $(T_I, (T_I - 2\,K))$. Therefore, the motional averaging model does not apply to the linear shift, while it does apply to the linear quadrupolar shift in N.M.R. experiments [8].

We may overcome the inconsistency of these results by assuming that for $\sphericalangle$ (**H**, **a**) = 4° 20′ and $T_I - 2\,K < T < T_I$, the phase fluctuations are too slow to fulfil the averaging conditions. Indeed, the energy differences involved in the linear shift are much larger than for **H//a**. A mean characteristic frequency of about 1.5×10^8 Hz is not sufficient to average the singularity positions for $\sphericalangle$ (**H**, **a**) = 4° 20′, although it is for **H//a** and *a fortiori* for N.M.R. experiments.

The local width parameter L_A^d (Fig. 7) exhibits the same qualitative feature as L_A^P (Fig. 4). This indicates

that both secular and non secular line broadenings due to amplitude fluctuations decrease on cooling as for a normal soft mode. On the other hand, the parameter L_ϕ^d (Fig. 7) is nearly stationary in the temperature range considered. Below ($T_I - 4$ K), L_ϕ^d and L_ϕ^P have nearly the same values.

It is worth noticing that the behaviours of L_A^d and L_ϕ^d compare to the behaviours of $T_{1,A}^{-1}$ and $T_{1,\phi}^{-1}$ respectively for ^{87}Rb [9]. Particularly $T_{1,\phi}^{-1}$ which corresponds to $\phi = \pm \frac{\pi}{2}$ and $\omega_L = 10^8$ Hz is stationary. This indicates that $J_{1,\phi}(\omega_L)$ is constant. In our case, the behaviour of L_ϕ^P indicates that $J_{1,\phi}(\langle \omega \rangle)$ increases from T_I to ($T_I - 4$ K).

Therefore, near T_I, we have to invoke a secular contribution to L_ϕ^d arising from large and slow fluctuations. Their decrease by cooling can be compensated for by the rise of nonsecular broadenings evidenced by L_ϕ^P.

To examine our results in the phason framework, let us introduce a gap $\omega_{\phi 0}$, a damping Γ_ϕ, and a dispersion $\omega_\phi^2 = \omega_{\phi_0}^2 + V_\phi^2(q - k_I)^2$ which is linear for a zero gap or quasi-linear for large $|\mathbf{q} - \mathbf{k}_I|$. The spectral density [9] is monitored by

$$J_{1,\phi}(\omega) \propto \mathrm{Im}\left\{\frac{\omega_{\phi_0}^2}{\omega^2} - 1 + i\frac{\Gamma_\phi}{\omega}\right\}^{1/2}$$

which is the sum of the contribution of modes within a sphere of the half-Brillouin zone $\left(R < \frac{\pi}{a}\right)$ centred at K_I. We have assumed an isotropic dispersion, $\Gamma_{\phi(q)} = \Gamma_\phi$ and $\omega_\phi(q = R) \gg \omega, \Gamma_\phi$. Im designates the imaginary part.

In K_2SeO_4 [16], inelastic neutron scattering has been consistently interpreted by assuming $\Gamma_\phi \simeq 3 \times 10^{11}$ s^{-1} and ω_{ϕ_0} in the range 10^{11} s^{-1}. These results hold for $(T_I - T) > 8$ K and for $|\mathbf{q} - \mathbf{k}_I| > 3 \times 10^{-2} |\mathbf{a}^*|$.

In Rb_2ZnCl_4, the relaxation time $T_{1,\phi}(^{87}Rb)$ [17], with $\omega_L \simeq 10^8$ s^{-1}, monitors the ratio $\Gamma_\phi/\omega_{\phi_0}$, which was found constant in the whole incommensurate phase, except near the lock-in transition at T_c. The increase of $T_{1,\phi}$ near T_c, was interpreted as a consequence of the multi-soliton regime, the phason mode being « acoustic-like » for $|q - k_I| < \frac{\pi}{b}$ and « optic-like » for $|q - k_I| > \frac{\pi}{b}$. b represents the distance between solitons which can be pinned to impurities and defects. As $T \to T_c$, b increases, and the phason transforms progressively into an intrinsic optic-like mode below T_c with a gap of about 10^{12} s^{-1}. By assuming that the damping parameter does not exhibit any drastic change from the incommensurate to the commensurate phase, the change of $T_{1,\phi}$ would indicate a gap ω_{ϕ_0} at about 10^{11} s^{-1} in the incommensurate phase.

E.P.R. measurements show a substantial non-

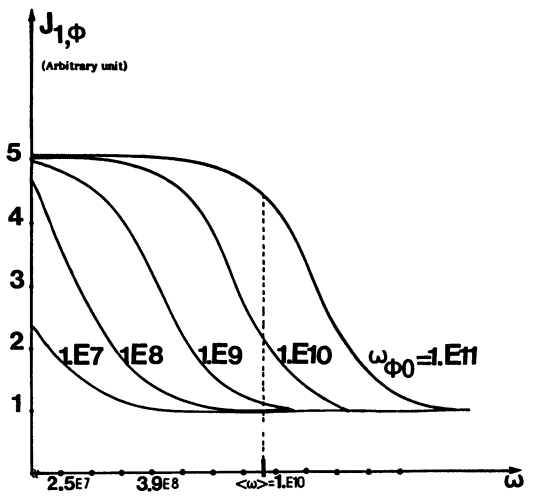

Fig. 8. — Graphs of the spectral density, $J_{1,\phi}$, of the phase fluctuations associated with a soft overdamped mode $\Gamma_\phi/\omega_{\phi_0} = 10$. Γ_ϕ and ω_{ϕ_0} represent respectively the damping parameter and the gap of the phason mode.

secular line broadening for $\phi = \frac{\pi}{2}$ — that is, a short $T_{1,\phi}$ arising from large $J_{1,\phi}(\langle \omega \rangle)$ below ($T_I - 4$ K). Setting $(\Gamma_\phi/\omega_{\phi_0}) = 10$ as a reasonable value for the overdamped phason, we obtain a large $J_{1,\phi}(\langle \omega \rangle)$ for $\omega_{\phi_0} > 10^{10}$ s^{-1}. Indeed, for $\omega_{\phi_0} < 10^{10}$ s^{-1}, $J_{1,\phi}(\langle \omega \rangle)$ would correspond to the wing of the spectral density curve and would be very low (Fig. 8). Therefore, below ($T_I - 4$ K) our results are consistent with an overdamped phase mode with a significant gap.

From ($T_I - 4$) K up to T_I, a sharp decrease of both Γ_ϕ and ω_{ϕ_0} would be necessary to account for the decrease $J_{1,\phi}(\langle \omega \rangle)$. Physically, a decrease of ω_{ϕ_0} can be associated with a depinning of the modulation wave. Indeed the local pinning potentials depend on the critical amplitude. A decrease of Γ_ϕ near the transition is unexpected, however, and the overdamped phason scheme does not hold. Obviously this model is not adapted to mirror the large phase fluctuations, pinning phenomena and floating modulation wave, occurring in this temperature range [6-8].

For the present time, avoiding any detailed explanation, we may invoke a « central peak » below T_I for the phase fluctuations, continuing the central peak for the ordering coordinate above T_I [15].

In any case, we believe that no definite explanation can be proposed without more experimental investigation of the spectral densities of phase fluctuations. The present work indicates the possibility of doing that by multiplying the E.P.R. measurements from S band (10^9 s^{-1}) to the Q band (3×10^{10} s^{-1}). Then the local measurements by N.M.R. and E.P.R. would permit coverage of the range 10^8-3×10^{10} s^{-1}, all of them being consistently based on the same principle : the modulation and the fluctuations of the quadrupolar spin lattice interaction. Of course, one has to assume that the Mn^{2+} probe is a neutral one.

References

[1] GESI, K., JIZUMI, M., *J. Phys. Soc. Japan* **46** (1979).

[2] QUILICHINI, M., PANNETIER, J., *Acta Cryst.* **B 39** (1983).

[3] ANDREWS, S. R., MASHIYAMA, M., *J. Phys. C* **16** (1983).

[4] AXE, J. D., JIZUMI, M., SHIRANE, G., *Phys. Rev.* **B 22** (1980).

[5] AXE, J. D., *Phys. Rev.* **B 21** (1980).

[6] BLINC, R., AILION, D. C., PRELOVSEK, P., RUTAR, V., *Phys. Rev. Lett.* **50** (1983).

[7] EMERY, J., HUBERT, S. et FAYET, J. C., *J. Physique Lett.* **45** (1984) L-693.

[8] BLINC, R., MILIA, F., TOPIC, B., ZUMER, S., *Phys. Rev.* **B 29** (1984).

[9] ZUMER, S. et BLINC, R., *J. Phys. C* **14** (1981).

[10] BLINC, R., AILION, D. C., DOLINSEK, J., ZUMER, S., *Phys. Rev. Lett.* **54** (1985).

[11] HEINE, V., MCCONNELL, J. D. C., *J. Phys. C* **17** (1983).

[12] KIND, R., *J. Mol. Structure* **111** (1983).

[13] BLINC, R., SELIGER, J., ZUMER, S. (to be published).

[14] PEZERIL, M., EMERY, J., FAYET, J. C., *J. Physique Lett.* **41** (1980).

[15] KAZIBA, A., PEZERIL, M., EMERY, J. et FAYET, J. C., *J. Physique Lett.* **46** (1985).

[16] QUILICHINI, M., CURRAT, R., Preprint submitted to *Solid State Commun.* (Sept.) 1983.

[17] BLINC, R., MILIA, F., RUTAR, V., ZUMER, S., *Phys. Rev. Lett.* **48** (1982).